Published in final edited form as:

J Pathol. 2013 January ; 229(1): 25–35. doi:10.1002/path.4114.

Physical and chemical microenvironmental cues orthogonally control the degree and duration of fibrosis-associated epithelial-to-mesenchymal transitions

Ashley C Brown[1], **Vincent F Fiore**[1], **Todd A Sulchek**[2,3], and **Thomas H Barker**[1,3,*]

[1]Wallace H Coulter Department of Biomedical Engineering, Georgia Institute of Technology and Emory University, Atlanta, GA, USA

[2]George W Woodruff School of Mechanical Engineering, Georgia Institute of Technology, Atlanta, GA, USA

[3]Parker H Petit Institute for Bioengineering and Biosciences, Georgia Institute of Technology, Atlanta, GA, USA

Abstract

Increased tissue stiffness and epithelial-to-mesenchymal transitions (EMTs) are two seemingly discrete hallmarks of fibrotic diseases. Despite recent findings highlighting the influence of tissue mechanical properties on cell phenotype, it remains unclear what role increased tissue stiffness has in the regulation of previously reported fibronectin-mediated EMTs associated with pulmonary fibrosis. Nano-indentation testing of lung interstitial spaces showed that in vivo cell-level Young's moduli increase with the onset of fibrosis from 2 to 17 kPa. In vitro, we found that stiff, but not soft, fibronectin substrates induce EMT, a response dependent on cell contraction-mediated integrin activation of TGFβ. Activation or suppression of cell contractility with exogenous factors was sufficient to overcome the effect of substrate stiffness. Pulse-chase experiments indicate that the effect of cell contractility is dose- and time-dependent. In response to low levels of TGFβ on soft surfaces, either added exogenously or produced through thrombin-induced contraction, cells will initiate the EMT programme, but upon removal revert to an epithelial phenotype. These results identify matrix stiffness and/or cell contractility as critical targets for novel therapeutics for fibrotic diseases.

Keywords

idiopathic pulmonary fibrosis; epithelial-to-mesenchymal transition; fibrosis; stiffness; cell contractility; alveolar epithelial cell

[*]Correspondence to: TH Barker, Wallace H Coulter Department of Biomedical Engineering, Georgia Institute of Technology and Emory University, 313 Ferst Drive, Suite 2108, Atlanta, GA 30332-0535, USA. thomas.barker@bme.gatech.edu.

Author contributions

ACB, VFF, TAS and THB designed research, analyzed and interpreted data and wrote the manuscript. ACB and VFF carried out experiments.

Introduction

Epithelial-to-mesenchymal transition (EMT) is a fundamental hallmark of fibrotic pathologies, where enhanced fibroblastic cellularity within scarring regions can originate from an epithelial origin [1,2]. EMT has been theorized to increase the number of extracellular matrix (ECM)-secreting mesenchymal cells perpetuating the fibrotic conditions and resulting in increased tissue stiffness; however, recent reports indicate that an increase in tissue stiffness may actually precede fibrotic responses [3]. It remains unclear precisely how tissue stiffness contributes to EMT in fibrosis. Understanding the relationship between, and course sequence of, tissue stiffness and EMT during fibrotic progression has major implications in how we approach these diseases therapeutically. Idiopathic pulmonary fibrosis (IPF), our experimental disease model, is a currently untreatable and ultimately fatal condition with 3 and 5 year mortality rates of 50% and 80%, respectively [4]. Although the exact mechanisms initiating lung fibrosis are poorly understood, recent studies implicate alveolar epithelial type II (ATII) cell EMT in the onset and progression of IPF [5–10].

EMT is a highly orchestrated process involving the integration of biochemical signals from ECM receptors (integrins) and growth factor receptors, such as transforming growth factor-β (TGFβ) receptor and receptor tyrosine kinases [11]. The ECM-associated growth factor TGFβ is highly implicated in EMT [6–10,12–16], and in the case of EMT associated with IPF, TGFβ appears to work in concert with provisional fibronectin (Fn) matrices, while alveolar epithelial cells (AECs) cultured on laminin (Ln) undergo apoptosis in the presence of TGFβ [8]. Furthermore, reports suggest that AECs will endocytose E-cadherin (E-cad) and undergo EMT when simply cultured on Fn, implicating the ECM protein as a constitutive driver of EMT [8,17]. Our previous studies employing recombinant fragments of Fn's cell binding domain suggest that Fn- mediated EMT responses by AECs are a consequence of integrin-specific engagement of the ECM [18].

Potentially adding to the complexity, numerous recent publications suggest that the physical/mechanical properties of the ECM, such as stiffness, can in part regulate a host of cellular processes and phenotypes, from regulation of stem cell differentiation to malignant phenotypes [19–24]. Specifically, cells are able to sense the underlying mechanical properties of the ECM, such as stiffness [25,26], and engage their actinomyosin contractile machinery in a manner that facilitates cell – ECM compliance matching [26,27]. As a consequence of this mechano-homeostasis between the cell and its ECM, cells in increasingly stiff environments display increased activation of contractile signals, such as Rho and Rho-associated kinase (ROCK), resulting in multiple and diverse secondary effects [21,28]. An elegant example of this was shown by Wipff *et al*. [29], who demonstrated that fibroblast integrin/force-mediated activation of TGFβ increases on increasingly stiff substrates, leading to greater myofibroblast differentiation on stiff substrates. This occurs via αv integrin binding to an RGD sequence to the prodomain, and the force-dependent conformational change of the latent complex, releasing active TGFβ [30]. These events have implications in the progression and treatment of fibrotic diseases; indeed, Barry-Hamilton *et al*. recently demonstrated successful reduction of bleomycin-induced pulmonary fibrosis in a murine model, along with a marked reduction in activated fibroblasts and decreased TGFβ signaling, by inhibiting the matrix crosslinking enzyme lysyl oxidase-like-2 [31].

AEC EMT has previously been shown to occur in response to stiff (ie coverglass or plastic) Fn surfaces through an integrin αvβ6/contraction-dependent TGFβ activation mechanism [8,17]. These reports suggest that Fn is a constitutive activator of EMT. We sought to expand upon these findings and determine the role of stiffness in Fn-mediated EMT. We hypothesized that as AECs engage increasingly stiff Fn substrates, they will become increasingly contractile, leading to enhanced TGFβ activation and EMT.

Materials and methods

Animals and bleomycin-induced fibrosis

C57/Bl6 mice (Charles River, MA, USA), 8–10 weeks old, were intubated and 3.2 U/kg bleomycin (EMD Chemicals, NJ, USA) was instilled intratracheally. The mice were sacrificed after 14 days for tissue harvesting. All experiments were performed in accordance with guidelines set forth by the National Institutes of Health (NIH) and Georgia Institute of Technology IACUC- approved protocols.

Lung tissue preparation

Lungs were inflated using 2% ultra-low-melting temperature agarose (SeaPrep, Lonza Inc.), warmed to 37°C and subsequently allowed to solidify on ice. The left lobe was dissected and 100 μm thick slices were generated, using a VT100S vibratome (Leica, IL, USA). The lung slices were stained with fluorescein- labelled lectin from the cry-baby tree, *Erythrina crystagalli* (ECL; Vector Laboratories), LysoTracker Red (Invitrogen) and Hoechst 33258 (Invitrogen) to visualize ATII, ATI and nuclei, respectively.

Atomic force microscopy (AFM) nano-indentation analysis

Micrographs were acquired using an inverted microscope (TiE, Nikon) as the AFM base (PlanFluor 20, 0.5 NA objective). For fibrotic regions, areas of enhanced cellularity distinct from larger airways were chosen. An MFP-3D-BIO AFM (Asylum Research) was used, with a 4.74 μm diameter silica glass bead customized-silicon nitride AFM tip (Veeco), and cantilever spring constants were determined using the thermal resonance frequency method, with values in the range 0.06–0.08 N/m. Force – indentation profiles were fitted to a Hertz model for elastic deformation between spheres to calculate the Young's modulus for each point, assuming a Poisson's ratio of 0.4. For single cell analysis, single force points were taken from at least five perinuclear regions that were >300 nm in height.

Cell culture

To determine the effect of substrate stiffness on ATII EMT, primary AECs or RLE-6TN cells were plated on polyacrylamide (PA) gels, with Fn crosslinked on the surface with the stiffness (*E*) 2, 8, 16, 24 or 32 kPA, or on glass coverslips coated with Fn or Ln as controls. PA gels of varying bisacrylamide concentrations were created on amino-silanated coverslips, as previously described [32]. Primary ATII cells were isolated from Sprague – Dawley male rats, as previously described [33], and plated immediately on PA gels or glass controls in Dulbecco's modified Eagle's medium (DMEM)/F12 medium with 10% fetal bovine serum (FBS) and incubated at 37°C and 5% CO2.

RLE-6TN cells were purchased from ATCC and grown in DMEM/F12 supplemented with 10% FBS and 1% penicillin/streptomycin (P/S). Cells were plated at a density of 100,000 cells/cm^2 in growth medium in the absence or presence of 10 μM Y-27632 (EMD Biosciences, Gibbstown, NJ, USA). To determine the role of contractility and/or TGFβ in stiffness-mediated EMT, the cells were cultured on soft substrates (2 kPa) in the presence of 0.5–4.0 U/ml thrombin (MP Biomedicals, CA, USA), 0.01–5 ng/ml active TGFβ (R&D Systems, Minneapolis, MN, USA) or 5 ng/ml TGFβ and 10 μg/ml TGFβ neutralizing antibody (9016, R&D Systems). In addition, cells were cultured on stiff substrates (32 kPa) in the presence of 10 μg/ml TGFβ neutralizing antibody or 10 μg/ml integrin αvβ6 inhibiting antibody (10D5, Millipore, Billerica, MA, USA). The medium was changed every 48 h. EMT events were analysed after 5 days in culture, because RLE- 6TN cells are known to undergo EMT in response to EMT-inducing stimuli in this time frame [34]. In dose – response/time-course experiments determining the role of TGFβ and thrombin in EMT induction on soft surfaces, EMT was also characterized after 2 days.

Immunofluorescence staining and circularity analysis

Following culture for 2 or 5 days, cells were fixed with 4% formaldehyde, permeabilized with 0.2% Triton- X 100, blocked with 10% goat serum and incubated overnight with anti-α-SMA (1A4, Sigma-Aldrich) or anti-E-cad (36/E-cadherin, BD Transduction Laboratories) antibodies. AlexaFluor 488-conjugated goat anti-mouse (Invitrogen) was used as the secondary anti- body. To characterize cell shape, actin was stained with Texas red/phalloidin (Invitrogen) and the nuclei were stained with Hoechst stain (Invitrogen). Samples were mounted in ProLong Gold antifade reagent (Invitrogen). Images were acquired with a Nikon TiE inverted fluorescence microscope (PlanFluor 20, 0.5 NA objective, 25°C) with a CoolSNAP HQ2 Monochromatic CCD camera. Circularity was determined using the equation: circularity = 4π(area/perimeter^2). Values closer to 1 indicate a more rounded cell.

Immunoblot

RLE-6TN cells were cultured for 5 days then lysed directly in Lamelli buffer containing protease and phosphatase inhibitors (Roche Applied Sciences). The samples were separated by electrophoresis, using a 4–15% gel, transferred to nitrocellulose using a semi-dry transfer system, blocked with 5% non-fat dried milk in Tris buffered saline (TBS), then incubated with E-cad (36/E-cadherin), pan cytokeratin (5D3 LP34, Abcam, Cambridge, MA, USA), α-SMA (1A4), prolyl- 4-hydroxylase (P4H; 1D3, Santa Cruz Biotechnology, Santa Cruz, CA, USA) or GAPDH (14C10, Cell Signaling Technology, Boston, MA, USA) antibodies overnight at 4°C. Following washing with TBS 0.1% Tween 20, the membranes were incubated for 2 h with IR secondary antibody (Licor), washed and then imaged, using the Odyssey IR scanner.

TGFβ activation assay

TGFβ activation was determined by the mink lung epithelial cell (MLEC) assay, as previously described [35]. Briefly, following 2 or 5 days of RLE-6TN culture, MLECs were seeded (50,000 cells/cm^2) on top of the RLE-6TN cells in serum-free DMEM/F12 medium 1% BSA in the absence or presence of contractility and TGFβ inducers/inhibitors. The cells were co-cultured for 16 h, lysed, and luciferase activity was determined via the One-Glo

luciferase assay (Promega). To determine levels of total TGFβ, samples were heated to 85°C for 10 min prior to plating of MLEC cells. Luminescence was measured using a Synergy H4 Multi-Mode Plate Reader (BioTek, Winooski, VT, USA). Luminescence values were normalized to MLECs cultured in the absence of TGFβ. Levels of active or total TGFβ activation were then calculated through interpolation, using a standard curve. The results presented were pooled from three independent triplicate experiments.

Statistical analysis

All statistical analysis for three or more experimental groups was performed by multivariate ANOVA, using Prism (Graphpad Software Inc., La Jolla, CA, USA). Statistical significance between groups was determined by performing Tukey's *posthoc* analysis. Statistical significance was achieved for $p < 0.05$.

Results

AECs experience significantly greater stiffness in fibrotic versus normal lung and primary ATII cells undergo EMT when cultured on Fn substrates of increasing stiffness

Given that one of the hallmarks of fibrotic diseases is an increase in tissue stiffness, we characterized the mechanical environment of the alveolus in normal and pathological conditions to determine the range of stiffness encountered by ATII cells *in vivo*. Intratracheal instillation of bleomycin was used to model pulmonary fibrosis in mice. As previously demonstrated [36], fixed lung sections isolated from fibrotic lung displayed increased cellularity and alveolar wall thickening, as observed through haematoxylin and eosin (H&E) staining compared to saline-treated mice (Figure 1A, B). Living lung slices were used for atomic force microscopy (AFM) nano-indentation testing of tissue elasticity. Lung tissue was tested within 6 h of harvest to ensure tissue integrity and resident cell via- bility; however, lung slices were found to remain viable for up to 48 h (see Supplementary material, Figure S1). Lung architecture observed in fixed tissues was recapitulated in thick (~100 μm) living lung slices, as observed by fluorescence microscopy of vital stains for ATI and ATII cells (inserts to Figure 1A, B). Mean and standard deviation (SD) values are reported for all samples (five mice/condition, n=180/mouse; Figure 1E); values for samples obtained from individual mice are presented in Figure S1. The average Young's modulus of normal lung tissue was 1.96 kPa (+/− 1.21) and in the bleomycin-treated mouse increased to 17.25 kPa (+/− 11.06). This is in agreement with previously published work exploring the microscale tissue mechanics of lung [37].

EMT has previously been observed *in vivo* in fibrotic lung regions of both human IPF patients and bleomycin-treated mice [8]. Because we observed a range of stiffness *in vivo* in fibrotic lung regions, we sought to determine whether increases in matrix/substrate stiffness alone would be sufficient to induce EMT. Using PA gels with surface-immobilized Fn and varying stiffness in the range 2–32 kPa, primary ATII cells were cultured for 5 days on PA gels or Fn- or Ln-coated glass and then analysed for EMT by immunofluorescence (IF) staining of actin, and epithelial and mesenchymal markers. Primary ATII cells cultured on lower-stiffness substrates (E=2 or 8 kPa) displayed a typical epithelial rounded morphology and diffuse cortical staining for actin, clear cell–cell borders observed through actin staining,

and minimal staining for α-SMA. In contrast, cells cultured on higher-stiffness substrates (E =16–32 kPa, Fn-coated glass) became elongated and displayed increasingly aligned, thick actin filaments characteristic of stress fibres, minimal staining for E-cad and positive staining for α-SMA-containing stress fibres (Figure 2A–U). E-cad staining was observed on 2 kPa surfaces at cell – cell contacts; however, staining at cell – cell contacts was less apparent on 8 kPa surfaces and E-cad was localized predominantly intracellularly. ATII cells have previously been shown to undergo EMT on Fn-coated glass surfaces (E~30 GPa) but maintain epithelial phenotypes on Ln-coated glass [8]. Using these conditions as control experiments, we observed identical results. Cell circularity was calculated to quantify differences observed in cell shape (Figure 1V) and decreased significantly with increasing substrate stiffness ($p < 0.001$). Freshly harvested cells expressed high levels of surfactant protein C (SPC), an ATII cell marker, and low levels of α-SMA (Figure 1W), indicating low levels of fibroblast contamination in the isolated cell population; however, small levels of fibroblast contamination can confound analysis of EMT. Therefore, an ATII cell line, RLE-6TN cells, which are widely utilized for studying ATII EMT events [6,12,34,38–40], was utilized for all remaining analyses. Like primary ATII cells, RLE-6TN cells underwent EMT on increasingly stiff Fn-surfaces but maintained an epithelial phenotype on Ln-glass surfaces (see Supplementary material, Figure S2).

Stiffness-mediated EMT is driven by increased contraction and integrin-mediated TGFβ activation

To characterize TGFβ activation, a mink lung epithelial reporter cell (MLEC) bioluminescence co-culture assay was performed (Figure 3A). RLE-6TN cells were found to increasingly activate TGFβ in response to increasing substrate stiffness, while total levels of TGFβ were similar on all PA gels (see Supplementary material, Figure S3A). As previously reported [29], we observed no significant differences in levels of MLEC's responsiveness to TGFβ in response to changes of substrate stiffness (unpublished data). As expected, control groups cultured on Fn-coated glass activated TGFβ to a significantly higher degree than those cultured on Ln-coated glass ($p < 0.01$). We also observed an increase in *Pai-1* mRNA expression by RLE-6TN cells in response to increasing substrate stiffness, further demonstrating a stiffness-dependent increase in active TGFβ (see Supplementary material, Figure S4). We then sought to correlate increased TGFβ activation with increased ATII cell stiffness, an indicator of cell contraction.

Using AFM nano-indentation testing, the average Young's modulus of individual cells was measured (Figure 3B); average cell stiffness increased with increasing substrate stiffness, reaching a maximum at approximately 6 kPa. Interestingly, cells on Ln-coated glass exhibited values similar to cells on soft Fn substrates, with average Young's moduli of approximately 1 kPa, suggesting that cellular stiffness matching is dependent on the ECM ligand. To determine the role of cell contractility in cellular stiffness matching, we measured the elasticity of cells on Fn-coated glass with the addition of 10 μM of the ROCK inhibitor Y-27632, and found that cell stiffness was decreased to levels similar to those observed on soft Fn substrates and Ln-coated glass.

To initially characterize the role of cell contractility in the observed stiffness-mediated EMT events, RLE-6TN cells were cultured for 5 days on substrates of varying stiffness in the presence of Y-27632, and EMT events were characterized. In the presence of Y-27632, cells maintained an epithelial morphology regardless of the underlying substrate (see Supplementary material, Figure S5). Inhibition of ROCK likely has global effects on many aspects of cell signalling, therefore we sought to more specifically con- firm that stiffness-mediated EMT of ATII cells is due to increased cell contractility and subsequent increased TGFβ activation. We analysed the EMT of ATII cells cultured for 5 days on soft substrates (E =2 kPa) in the presence of 5 ng/ml active TGFβ, 0.5 U/ml of the contractility agonist thrombin, or a combination of thrombin and TGFβ-neutralizing antibodies. In addition to thrombin's direct proteolytic activation of TGFβ at concentrations >5 U/ml [29,41], it has also been shown to lead to non-proteolytic integrin-mediated activation of TGFβ through binding to PAR1 [42]. Conversely, cells were cultured on stiff substrates (E =32 kPa) in the presence of TGFβ-neutralizing antibodies or integrin αvβ6 function-blocking antibodies to prevent integrin-mediated mechanoactivation of TGFβ. In the presence of active TGFβ or thrombin, cells cultured on soft substrates displayed a predominantly mesenchymal phenotype (Figure 3C, D, H, I, M, N, R, T), while cells cultured in the presence of both thrombin and TGFβ-neutralizing antibodies displayed a predominantly epithelial phenotype (Figure 3E, J, O, R, T). The converse was observed on stiff substrates in the presence of TGFβ- or integrin αvβ6-neutralizing antibodies, with cells presenting a predominantly epithelial morphology (Figure 3F, G, K, L, P, Q, S, T). These data indicate that contractility-induced EMT involves TGFβ signaling. However, in addition to inducing contractility, thrombin signals through additional pathways that could account, in part, for some of the subtle differences in phenotype compared to those observed in response to exogenous TGFβ. To characterize the role of TGFβ activation in the observed events, the MLEC bioluminescence co-culture assay was performed (Figure 3U). Cells cultured on soft gels in the presence of thrombin- activated TGFβ significantly more than under soft control conditions (p <0.001). As a control, further addition of TGFβ-neutralizing antibodies abrogated the thrombin-induced enhanced TGFβ signal. In addition, cells cultured on stiff gels in the presence of either TGFβ- or integrin-αvβ6-neutralizing antibodies resulted in an abrogation of active TGFβ. To further characterize the role of thrombin in integrin-mediated TGFβ activation, and to rule out possible proteolytic activation of TGFβ by thrombin, cells were cultured on soft substrates in the presence of both thrombin and integrin αvβ6-neutralizing antibodies and were found to display a predominantly epithelial phenotype (see Supplementary material, Figure S6). To determine whether stiffness affects TGFβ receptor activation, cells were cultured on either soft or stiff surfaces in the presence of exogenously added active TGFβ and integrin-αvβ6-neutralizing antibodies and were found to display predominantly mesenchymal phenotypes on soft surfaces and robust mesenchymal phenotypes on stiff surfaces (Figure S6).

An acute 'pulse' of active TGFβ, but not the contractility agonist thrombin, is sufficient to induce EMT on soft surfaces

To determine the relative time course of events, a pulse- chase experiment was performed with cells cultured on soft gels. ATII cells were pulsed with 5 ng/ml active TGFβ or 0.5 U/ml thrombin for 48 h, followed by chasing with standard media for 3 days, thus

recapitulating the time of the original EMT experiments. EMT was then analysed. Cells pulsed with TGFβ were found to undergo EMT (Figure 4A, C, E, G, H). Furthermore, blocking additional residual matrix-bound TGFβ signalling through the addition of a TGFβ-inhibiting antibody after the TGFβ pulse resulted in cells with a predominantly mesenchymal morphology; however, cells cultured under these conditions began to regain CK expression (see Supplementary material, Figure S7). In contrast, cells pulsed with thrombin for 2 days displayed an epithelial morphology on day 5 (Figure 4B, D, F–H). These data suggest that a minimum level of TGFβ signalling may be required to initiate the EMT programme and that only a sustained contraction of ECs is capable of achieving this threshold. Cell stiffness was measured to determine whether the addition of thrombin or active TGFβ results in an increase in cell stiffness, either acutely or in the long term. Cells were cultured overnight on soft substrates in the presence or absence of TGFβ or thrombin, and cell stiffness was found to significantly increase in the presence of either stimulant compared to cells cultured in standard medium alone ($p < 0.05$). Interestingly, upon removal of the cell culture additives, cells initially incubated with thrombin exhibited a decrease in single cell stiffness over the course of 3 days; however, cells initially incubated with TGFβ maintained the increase in cell stiffness over the time course and did not return to basal levels (Figure 4I).

Induction of EMT events on soft substrates by TGFβ or thrombin pulse is dose-dependent

To further elucidate the role of TGFβ and sustained contraction in the induction of EMT, EMT was characterized in response to varying levels of TGFβ and thrombin after 2 or 5 days in culture. RLE-6TN cells were cultured on soft substrates in the presence of varying levels of either active TGFβ (0.01, 0.1 or 5 ng/ml) or thrombin (0.5, 1 or 4 U/ml) for the initial 48 h and then in media with (continuous) or without (pulse) these same additives for 3 additional days (Figure 5). The levels of TGFβ chosen were based on the amount of TGFβ activated by RLE-6TN cells in the presence of 0.5 U/ml thrombin in previous experiments. EMT events were then analysed at 2 or 5 days, as before. It was found that after 2 or 5 days in culture with continuous exposure to TGFβ or thrombin, cells displayed a predominantly mesenchymal phenotype.

Cells pulsed with 4 U/ml thrombin, like cells pulsed with 5 ng/ml of TGFβ (Figure 4), were found to maintain a mesenchymal phenotype at day 5. However, cells pulsed with low levels of TGFβ (0.01 ng/ml), similarly to cells pulsed with low levels of thrombin (0.5 U/ml; Figure 4), reverted to a predominantly epithelial phenotype (Figure 5BB, JJ, RR, UU–WW). Cells pulsed with intermediate doses (1 U/ml thrombin or 0.1 ng/ml TGFβ) displayed a mixed phenotype on day 5. These data strongly suggest that while low levels of TGFβ signalling can initiate an EMT programme with continuous exposure, a threshold is required to maintain the EMT programme after removal of TGFβ. Below that critical threshold, EMT can be reversed on soft substrates. It was also found that cells increasingly activated TGFβ in response to increasing concentrations of thrombin (Figure 5V). As expected, addition of exogenous active TGFβ resulted in a dose- dependent increase in the observed levels of active TGFβ. Amounts of both active and total TGFβ were lower after 5 days compared to identical conditions after 48 h, except with the addition of 5 ng/ml TGFβ, which produced

similar values of approximately 10 ng/ml for both time points (see Supplementary material, Figure S3B).

Discussion

This study strongly suggests that there is a delicate balance between ECM stiffness, TGFβ and EMT and identifies matrix stiffness and increased cell contractility as important targets for fibrotic disease therapeutics. We demonstrate that increased epithelial cell contraction on stiff Fn-surfaces leads to integrin-mediated TGFβ activation and spontaneous EMT. Furthermore, dose–response pulse-chase experiments demonstrate that either high concentrations of active TGFβ for short periods of time, or low levels of TGFβ for an extended period of time, e.g. via integrin-mediated activation, lead to sustained EMT. However, in response to low levels of TGFβ, either added endogenously or activated through increased contraction, cells will initiate the EMT programme but, upon removal, will revert to an epithelial phenotype. These data suggest that if matrix stiffness associated with fibrotic conditions could be treated and alleviated, aberrant EMT-derived mesenchymal cells could potentially revert to a normal phenotype. Furthermore, there appears to be a governing equation involving the amplitude of the TGFβ signal and the length of TGFβ exposure time that defines the probability of an epithelial cell presenting a mesenchymal phenotype.

The origins of increased matrix stiffness in fibrosis are unclear, but potentially emanate from residential cell populations and/or the over-production or activation of crosslinking enzymes. Fibroblasts that have differentiated down a contractile, myofibroblastic pathway are known to exhibit significant contractile force [29]. Such cell-derived forces are capable of stressing the surrounding ECM, leading to increased microenvironmental stiffness. Additionally, recent evidence suggests that even normal fibroblast subpopulations, as in the case of Thy-1 surface expression, may display significant differences in their capacity to exert force on their matrix [43,44]. Reports have shown that lysyl oxidase in the tumour microenvironment is sufficient to crosslink and stiffen tumour stroma [45], and transglutaminases have long been known to catalyse ECM crosslinking and have recently been shown to result in tissue stiffening [46]. Inhibiting pro-fibrotic cellular contraction, lysyl oxidases and/or transglutaminases would be hypothesized to inhibit EMT *in vivo* and could serve as a successful therapeutic approach for IPF and other fibrotic diseases.

Our findings, along with those of others, suggest that therapeutic approaches to EMT-related diseases that focus on the cell only are likely flawed. The pathological extracellular microenvironment is capable of presenting pro-fibrotic signals that ensure the progression of the disease despite any acute eradication of the resident transformed cells. How one modifies the biochemical and biophysical microenvironment will likely be a greater determinant in the success of future therapeutics.

Supplementary Material

Refer to Web version on PubMed Central for supplementary material.

Acknowledgments

The authors would like to thank Wenwei Xu for assistance with AFM, Marilyn Markowski and Alison Douglas for assistance with primary ATII cell isolation, and Justin Chen for assistance with PA gel characterization. Funding was provided by the NSF ERC Georgia Tech/Emory Tissue Engineering Center (GTEC; EEC-9731643) to THB, NIH T32-GM008433 to ACB, and NSF GRFP to VFF (NSF10604).

References

1. Iwano M, Plieth D, Danoff TM, et al. Evidence that fibroblasts derive from epithelium during tissue fibrosis. J Clin Invest. 2002; 110:341–350. [PubMed: 12163453]
2. Coward WR, Saini G, Jenkins G. The pathogenesis of idiopathic pulmonary fibrosis. Ther Adv Respir Dis. 2010; 4:367–388. [PubMed: 20952439]
3. Georges PC, Hui JJ, Gombos Z, et al. Increased stiffness of the rat liver precedes matrix deposition: implications for fibrosis. Am J Physiol Gastrointest Liver Physiol. 2007; 293:G1147–1154. [PubMed: 17932231]
4. Spruit MA, Janssen DJ, Franssen FM, et al. Rehabilitation and palliative care in lung fibrosis. Respirology. 2009; 14:781–787. [PubMed: 19703060]
5. Selman M, Pardo A. Role of epithelial cells in idiopathic pulmonary fibrosis: from innocent targets to serial killers. Proc Am Thorac Soc. 2006; 3:364–372. [PubMed: 16738202]
6. Willis BC, Liebler JM, Luby-Phelps K, et al. Induction of epithelial – mesenchymal transition in alveolar epithelial cells by transforming growth factor-β1: potential role in idiopathic pulmonary fibrosis. Am J Pathol. 2005; 166:1321–1332. [PubMed: 15855634]
7. Kasai H, Allen JT, Mason RM, et al. TGF-β1 induces human alveolar epithelial to mesenchymal cell transition (EMT). Respir Res. 2005; 6:56. [PubMed: 15946381]
8. Kim KK, Kugler MC, Wolters PJ, et al. Alveolar epithelial cell mesenchymal transition develops *in vivo* during pulmonary fibrosis and is regulated by the extracellular matrix. Proc Natl Acad Sci USA. 2006; 103:13180–13185. [PubMed: 16924102]
9. Xu J, Lamouille S, Derynck R. TGFβ-induced epithelial to mesenchymal transition. Cell Res. 2009; 19:156–172. [PubMed: 19153598]
10. Wynn TA. Cellular and molecular mechanisms of fibrosis. J Pathol. 2008; 214:199–210. [PubMed: 18161745]
11. Thiery JP, Sleeman JP. Complex networks orchestrate epithelial – mesenchymal transitions. Nat Rev Mol Cell Biol. 2006; 7:131–142. [PubMed: 16493418]
12. Jain R, Shaul PW, Borok Z, et al. Endothelin-1 induces alveolar epithelial – mesenchymal transition through endothelin type A receptor-mediated production of TGFβ1. Am J Respir Cell Mol Biol. 2007; 37:38–47. [PubMed: 17379848]
13. Lamouille S, Derynck R. Cell size and invasion in TGFβ-induced epithelial to mesenchymal transition is regulated by activation of the mTOR pathway. J Cell Biol. 2007; 178:437–451. [PubMed: 17646396]
14. Lenferink AE, Magoon J, Cantin C, et al. Investigation of three new mouse mammary tumor cell lines as models for transforming growth factor (TGF)β and Neu pathway signaling studies: identification of a novel model for TGFβ-induced epithelial-to-mesenchymal transition. Breast Cancer Res. 2004; 6:R514–530. [PubMed: 15318933]
15. Park SH, Choi MJ, Song IK, et al. Erythropoietin decreases renal fibrosis in mice with ureteral obstruction: role of inhibiting TGFβ-induced epithelial-to-mesenchymal transition. J Am Soc Nephrol. 2007; 18:1497–1507. [PubMed: 17389738]
16. Masszi A, Fan L, Rosivall L, et al. Integrity of cell – cell contacts is a critical regulator of TGFβ1-induced epithelial-to-myofibroblast transition: role for β-catenin. Am J Pathol. 2004; 165:1955–1967. [PubMed: 15579439]
17. Kim Y, Kugler MC, Wei Y, et al. Integrin α3β1-dependent β-catenin phosphorylation links epithelial Smad signaling to cell contacts. J Cell Biol. 2009; 184:309–322. [PubMed: 19171760]
18. Brown AC, Rowe JA, Barker TH. Guiding epithelial cell phenotypes with engineered integrin-specific recombinant fibronectin fragments. Tissue Eng A. 2011; 17:139–150.

19. Engler AJ, Griffin MA, Sen S, et al. Myotubes differentiate optimally on substrates with tissue-like stiffness: pathological implications for soft or stiff microenvironments. J Cell Biol. 2004; 166:877–887. [PubMed: 15364962]
20. Engler AJ, Sen S, Sweeney HL, et al. Matrix elasticity directs stem cell lineage specification. Cell. 2006; 126:677–689. [PubMed: 16923388]
21. Paszek MJ, Zahir N, Johnson KR, et al. Tensional homeostasis and the malignant phenotype. Cancer Cell. 2005; 8:241–254. [PubMed: 16169468]
22. Wozniak MA, Desai R, Solski PA, et al. ROCK-generated contractility regulates breast epithelial cell differentiation in response to the physical properties of a three-dimensional collagen matrix. J Cell Biol. 2003; 163:583–595. [PubMed: 14610060]
23. Pelham RJ Jr, Wang Y. Cell locomotion and focal adhesions are regulated by substrate flexibility. Proc Natl Acad Sci USA. 1997; 94:13661–13665. [PubMed: 9391082]
24. Pelham RJ Jr, Wang YL. Cell locomotion and focal adhesions are regulated by the mechanical properties of the substrate. Biol Bull. 1998; 194:348–349. discussion, 349–350. [PubMed: 11536880]
25. Vogel V, Sheetz M. Local force and geometry sensing regulate cell functions. Nat Rev Mol Cell Biol. 2006; 7:265–275. [PubMed: 16607289]
26. Georges PC, Janmey PA. Cell type-specific response to growth on soft materials. J Appl Physiol. 2005; 98:1547–1553. [PubMed: 15772065]
27. Solon J, Levental I, Sengupta K, et al. Fibroblast adaptation and stiffness matching to soft elastic substrates. Biophys J. 2007; 93:4453–4461. [PubMed: 18045965]
28. Fan L, Sebe A, Peterfi Z, et al. Cell contact-dependent regulation of epithelial –myofibroblast transition via the rho–rho kinase–phospho–myosin pathway. Mol Biol Cell. 2007; 18:1083–1097. [PubMed: 17215519]
29. Wipff PJ, Rifkin DB, Meister JJ, et al. Myofibroblast contraction activates latent TGFβ1 from the extracellular matrix. J Cell Biol. 2007; 179:1311–1323. [PubMed: 18086923]
30. Shi M, Zhu J, Wang R, et al. Latent TGFβ structure and activation. Nature. 2011; 474:343–349. [PubMed: 21677751]
31. Barry-Hamilton V, Spangler R, Marshall D, et al. Allosteric inhibition of lysyl oxidase-like-2 impedes the development of a pathologic microenvironment. Nat Med. 2010; 16:1009–1017. [PubMed: 20818376]
32. Tse JR, Engler AJ. Preparation of hydrogel substrates with tunable mechanical properties. Curr Protoc Cell Biol. 2010; 10(unit 10–16)
33. Annes JP, Chen Y, Munger JS, et al. Integrin αVβ6-mediated activation of latent TGFβ requires the latent TGFβ binding protein- 1. J Cell Biol. 2004; 165:723–734. [PubMed: 15184403]
34. Felton VM, Borok Z, Willis BC. *N*-acetylcysteine inhibits alveolar epithelial – mesenchymal transition. Am J Physiol Lung Cell Mol Physiol. 2009; 297:L805–812. [PubMed: 19648289]
35. Abe M, Harpel JG, Metz CN, et al. An assay for transforming growth factor-β using cells transfected with a plasminogen activator inhibitor-1 promoter – luciferase construct. Anal Biochem. 1994; 216:276–284. [PubMed: 8179182]
36. Lovgren AK, Jania LA, Hartney JM, et al. COX-2-derived prostacyclin protects against bleomycin-induced pulmonary fibrosis. Am J Physiol Lung Cell Mol Physiol. 2006; 291:L144–156. [PubMed: 16473862]
37. Liu F, Mih JD, Shea BS, et al. Feedback amplification of fibrosis through matrix stiffening and COX-2 suppression. J Cell Biol. 2010; 190:693–706. [PubMed: 20733059]
38. Xu GP, Li QQ, Cao XX, et al. Effect of Smad7 on transforming growth factor-β1-induced alveolar epithelial to mesenchymal transition. Zhonghua Yi Xue Za Zhi. 2007; 87:1918–1923. [PubMed: 17923018]
39. Aoyagi-Ikeda K, Maeno T, Matsui H, et al. Notch induces myofibroblast differentiation of alveolar epithelial cells via transforming growth factor-β-Smad3 pathway. Am J Respir Cell Mol Biol. 2011; 45:136–144. [PubMed: 21749980]
40. Zhou G, Dada LA, Wu M, et al. Hypoxia-induced alveolar epithelial – mesenchymal transition requires mitochondrial ROS and hypoxia-inducible factor 1. Am J Physiol Lung Cell Mol Physiol. 2009; 297:L1120–1130. [PubMed: 19801454]

41. Taipale J, Koli K, Keski-Oja J. Release of transforming growth factor-β1 from the pericellular matrix of cultured fibroblasts and fibrosarcoma cells by plasmin and thrombin. J Biol Chem. 1992; 267:25378–25384. [PubMed: 1281156]

42. Jenkins RG, Su X, Su G, et al. Ligation of protease-activated receptor 1 enhances αvβ6 integrin-dependent TGFβ activation and promotes acute lung injury. J Clin Invest. 2006; 116:1606–1614. [PubMed: 16710477]

43. Barker TH, Grenett HE, MacEwen MW, et al. Thy-1 regulates fibroblast focal adhesions, cytoskeletal organization and migration through modulation of p190 RhoGAP and Rho GTPase activity. Exp Cell Res. 2004; 295:488–496. [PubMed: 15093746]

44. Zhou Y, Hagood JS, Lu B, et al. Thy-1-integrin αvβ5 interac- tions inhibit lung fibroblast contraction-induced latent transforming growth factor-β1 activation and myofibroblast differentiation. J Biol Chem. 285:22382–22393.

45. Levental KR, Yu H, Kass L, et al. Matrix crosslinking forces tumor progression by enhancing integrin signaling. Cell. 2009; 139:891–906. [PubMed: 19931152]

46. Santhanam L, Tuday EC, Webb AK, et al. Decreased *S* - nitrosylation of tissue transglutaminase contributes to age-related increases in vascular stiffness. Circ Res. 2010; 107:117–125. [PubMed: 20489165]

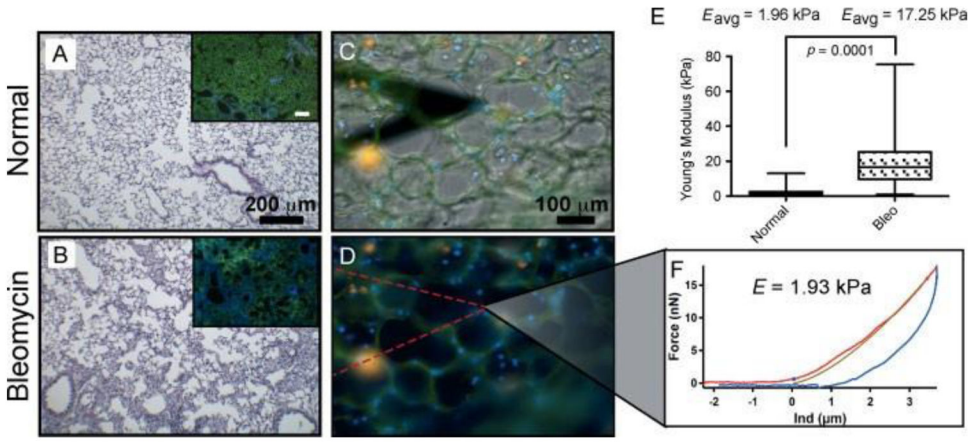

Figure 1.

Lung slices from mice exposed to bleomycin display higher Young's moduli than those from healthy mice. H&E staining was performed on normal and bleomycin-treated lung sections (A, B) and living lung slices were imaged using vital stains for ATI and ATII cells (A, B, inserts). The average Young's modulus of the lung tissue was measured with AFM. Representative DIC-vital stain fluorescence overlay (normal tissue; C), vital stain fluorescence-only images (D) used to guide the position of the AFM tip, and a force – indentation profile (F) for the depicted region are shown. Mean and SD values are reported (E).

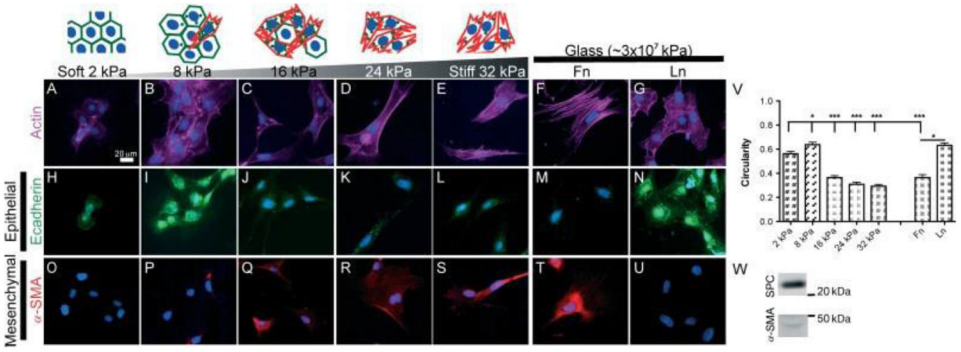

Figure 2.

Primary ATII cells undergo EMT on increasingly stiff Fn surfaces. Primary ATII cells were isolated and cultured on Fn –PA gels or on Fn- or Ln-coated glass for 5 days, and EMT responses analysed through changes in actin cytoskeleton alignment and cell circularity (A–G, V) and through IF staining for E-cad (H–N) and α-SMA (O–U). To demonstrate the purity of isolated ATII cells, levels of SPC and α-SMA in freshly isolated cells were determined through western blotting (W). Experiments were performed in triplicate; representative images are presented; ***$p < 0.001$, *$p < 0.05$.

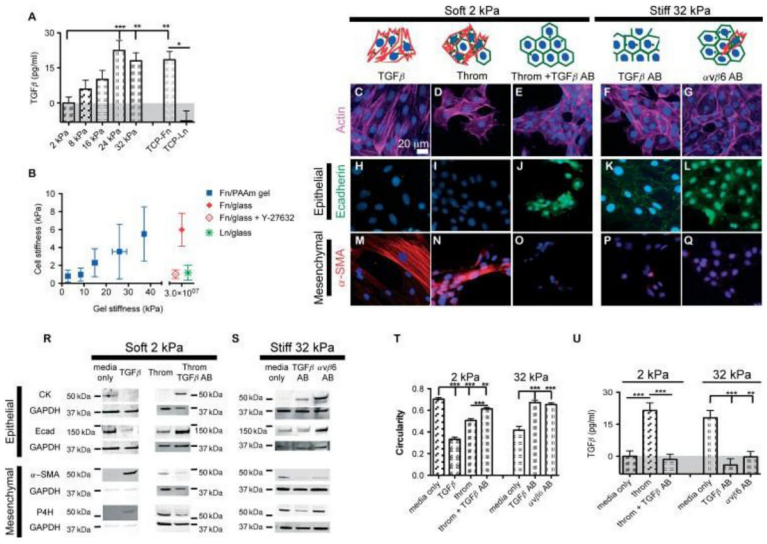

Figure 3.

Stiffness-mediated EMT is driven by increased contraction and integrin-mediated TGFβ activation. RLE-6TN cells were cultured for 5 days on substrates of increasing stiffness and levels of TGFβ activation were determined, using the MLEC bioluminescence co-culture assay (A). Single cell elasticity was measured with AFM nano-indentation to characterize cell stiffening in response to substrate stiffness and/or ECM ligand (B). Averages of cell stiffness and stiffness for each gel mixture are presented. RLE-6TN cells were also cultured for 5 days on soft substrates (2 kPA) in the presence of active TGFβ (C, H, M), the contractility agonist thrombin (D, I, N), or thrombin and TGFβ-neutralizing antibodies (E, J, O) or on stiff substrates (32 kPA) in the presence of TGFβ- (F, K, P) or integrin αvβ6-neutralizing antibodies (G, L, Q). EMT events were analysed though changes in actin cytoskeleton alignment and cell circularity (C–G, T) and changes in epithelial and mesenchymal protein expression through IF staining for E-cad (H–L) and α-SMA (M–Q) and western blotting for E-cad, CK, α-SMA, P4H and GAPDH (R, S). A minimum of three independent experiments were performed; representative images are presented. TGFβ activation was determined through a MLEC bioluminescence co-culture assay (U). $^{**}p < 0.01$, $^{***}p < 0.001$.

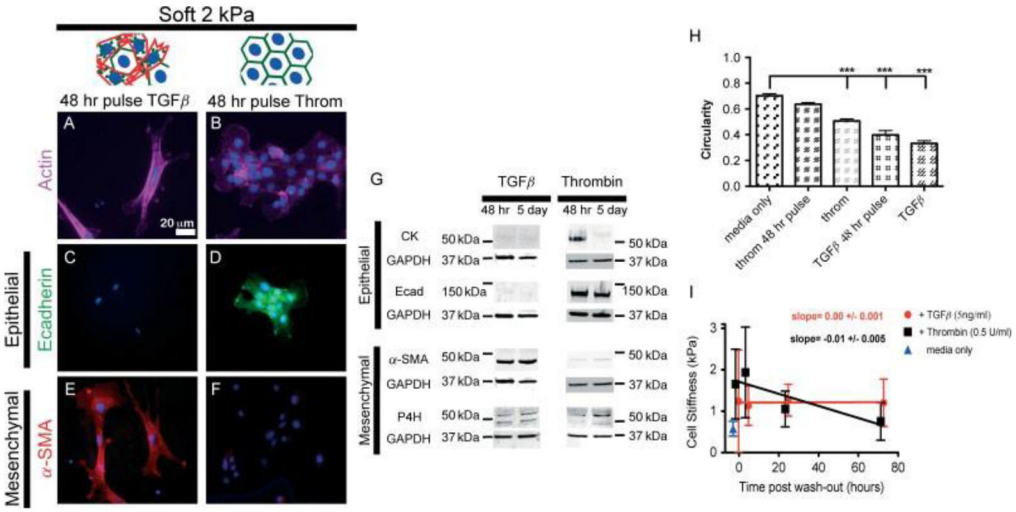

Figure 4.

Induction of EMT events on soft substrates is achieved with a TGFβ pulse but not a thrombin pulse. RLE-6TN cells were cultured for 5 days on soft substrates (2 kPA) in the presence of either 5 ng/ml active TGFβ (A, C, E) or 0.5 U/ml thrombin (B, D, F) for the initial 48 h and then media without additives for 3 additional days. EMT events were analysed though changes in actin cytoskeleton alignment and cell circularity (A, B, H), changes in epithelial and mesenchymal protein expression through IF staining for Ecad (C, D) and α-SMA (E, F) and western blotting for E-cad, CK, α-SMA, P4H and GAPDH (G). Experiments were performed a minimum of three times; representative images are presented. Single cell elasticity was measured via AFM force mapping to characterize cell stiffening on 2 kPa surfaces in response to an overnight stimulation with either active TGFβ or thrombin and 3, 24 and 72 h after washout (I). $*p < 0.05$, $**p < 0.01$, $***p < 0.001$.

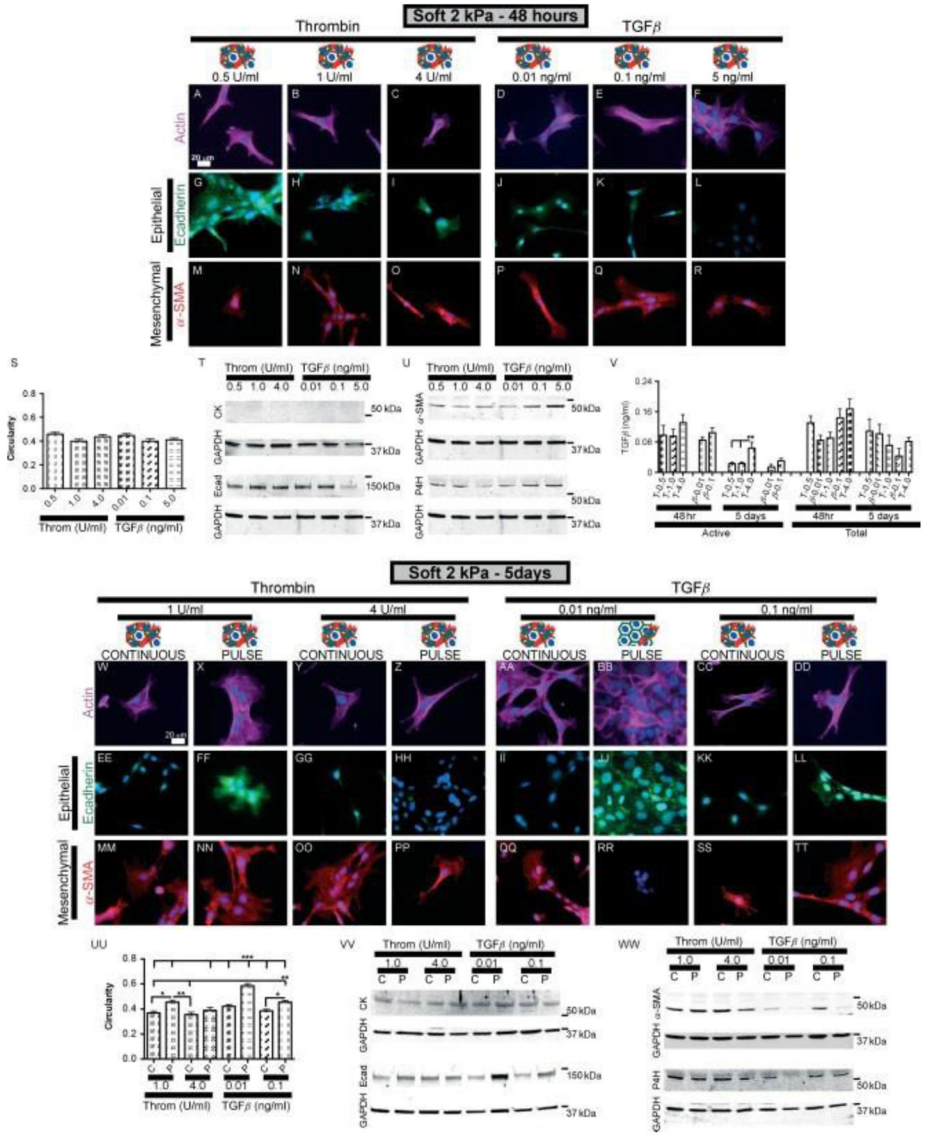

Figure 5.

Induction of EMT events on soft substrates by a TGFβ or thrombin pulse is dose-dependent. RLE-6TN cells were cultured for 5 days on soft substrates (2 kPa) in the presence of varying levels of active TGFβ (0.01, 0.1 or 5 ng/ml) or thrombin (0.5, 1 or 4 U/ml) for the initial 48 h and then media with or without additives for 3 additional days. EMT events were analysed at 48 h (A–U) or 5 days (W–WW) through changes in actin cytoskeleton alignment and cell circularity (A–F, S, W–DD, UU), changes in epithelial and mesenchymal protein expression through IF staining for E-cad and α-SMA (G–R, EE–TT) and western blotting for E-cad, CK, α-SMA, P4H and GAPDH (T, U, VV, WW). Experiments were performed in triplicate; representative images are presented. Levels of active and total TGFβ were determined through a MLEC bioluminescence co-culture assay. T, thrombin; β, TGFβ (V). $*p < 0.05$, $**p < 0.01$, $***p < 0.001$.